Drug delivery

DOI: 10.1002/smll.200700807

Multifunctional Nanoparticles for Photothermally Controlled Drug Delivery and Magnetic Resonance Imaging Enhancement**

*Huiyul Park, Jaemoon Yang, Sungbaek Seo, Kyujung Kim, Jinsuk Suh, Donghyun Kim, Seungjoo Haam, and Kyung-Hwa Yoo**

Recently, near-infrared (NIR) resonant nanomaterials such as gold nanoshell particles,[1–6] hollow Au nanoshells,[7,8] and Au nanorods[9,10] have been extensively studied for promising applications in biomedicine, because optical transmission through tissues is optimal in the NIR region (800–1200 nm). These nanomaterials strongly absorb NIR light and convert it into heat; thus, they can be utilized for photothermal therapy. Indeed, Hirsh et al.[3] demonstrated that silica/Au nanoshell particles could be used to deliver a therapeutic dose of heat to kill targeted cells without damaging normal cells because of excessive local heating. Furthermore, Au nanoshells were also combined with magnetic nanoparticles and cancer-cell-specific antibodies to develop a multifunctional platform for simultaneous diagnosis via magnetic resonance imaging (MRI) and NIR photothermal therapy.[11]

Photothermal conversion in Au nanoshells increases the temperature locally; elevated temperature can sensitize targeted cells to cytotoxic agents by increasing membrane permeability and blood vessel dilation.[12] Therefore, if the photothermal therapy is combined with chemotherapy, a much higher therapeutic efficacy is expected. In a previous study,[4] poly(N-isopropylacrylamide-*co*-acrylamide) (poly(NIPAAm-*co*-AAm))–Au/Au_2S nanoshell composites containing methylene blue, ovalbumin, or bovine serum albumin (BSA) were synthesized, and the drug release from these composites was reported to be enhanced upon NIR irradiation. However, NIPAAm-*co*-AAm hydrogels, which undergo a reversible phase transition in response to NIR irradiation, are not appropriate for drug delivery because of their toxicity.

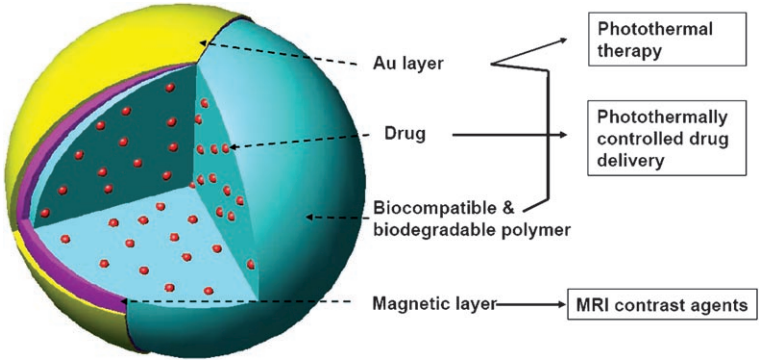

Figure 1. Schematic diagram of drug-loaded polymer–metal multilayer H-S NPs. The drug is loaded into biocompatible and biodegradable polymer nanoparticles, and magnetic and Au layers are deposited on the polymer nanoparticles. These nanoparticles provide multiple functions, such as photothermal therapy, photothermally controlled drug delivery, and MRI contrast enhancement.

Thus, we herein propose biodegradable polymer–metal multilayer half-shell nanoparticles (H-S NPs) for drug delivery, as shown in Figure 1. The drug is encapsulated within biocompatible and biodegradable polymer nanoparticles, and metal multilayers are deposited on these nanoparticles. Since the physical deposition method yields half-shells, the drug is released through the open half of the shell, the interior of which is now exposed. Moreover, since these nanoparticles are NIR resonant and the drug release from polymer nanoparticles is accelerated by increasing the temperature,[13] it would be possible to modulate the rate of drug release in response to NIR irradiation. In this study, we have fabricated poly(lactic-*co*-glycolic acid) (PLGA)–Au H-S NPs and PLGA–Mn/Au H-S NPs containing rhodamine as a model drug and demonstrated their use for photothermally controlled drug delivery and MRI enhancement.

Figure 2a shows the absorption spectra measured by using a UV-visible/NIR spectrometer for PLGA–Au H-S NPs having different Au shell thickness. In spite of the asymmetric geometry, these absorption peaks are located in the NIR region, in agreement with the results reported for

[*] H. Park, Prof. K.-H. Yoo
Department of Physics
Yonsei University
Seoul 120-742 (Korea)
Fax: (+82) 231-270-90
E-mail: khyoo@yonsei.ac.kr
J. Yang, S. Seo, S. Haam
Department of Chemical Engineering
Yonsei University
Seoul 120-742 (Korea)
K. Kim, Prof. D. Kim
Department of Electrical and Electronic Engineering
Yonsei University
Seoul 120-742 (Korea)
Prof. J. Suh
Department of Radiology, College of Medicine
Yonsei University
Seoul 120-752 (Korea)

[**] This work has been financially supported by the Korea Science and Engineering Foundation through the National Core Research Center for Nanomedical Technology (Grant No. R15-20040924-00000-0).

Supporting Information is available on the WWW under http://www.small-journal.com or from the author.

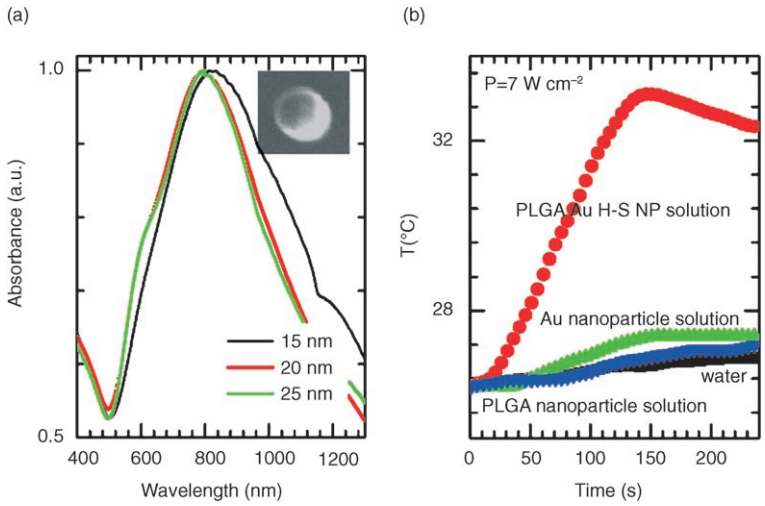

Figure 2. a) Visible/NIR spectra for PLGA–Au H-S NPs with different Au shell thickness. The inset is a field-emission scanning electron microscopy (FESEM) image of the PLGA–Au H-S NPs. b) Temperature versus time for the PLGA–Au H-S NP solution (145 μg mL^{-1}), the Au nanopraticle solution (2.7 mg mL^{-1}), the PLGA nanoparticle solution (3.3 mg mL^{-1}), and the deionized water irradiated by the 808-nm laser diode with a power density of 7 W cm^{-2} from 0 to 120 s, but turned off from 120 to 240 s.

silica–Au nanoshell particles.[1] However, the peak positions are barely affected by altering the Au shell thickness, probably because of the nonhomogenous size distribution of the PLGA nanoparticles (see below, Figure 4).

The NIR absorption peak indicates that NIR light is absorbed by PLGA–Au H-S NPs and converted into thermal energy via electron–phonon and phonon–phonon interactions.[3,4] In order to investigate this photothermal conversion property, the temperature of the PLGA–Au H-S NP solution was measured using a thermocouple while the solution was irradiated with NIR light, with a laser diode of wavelength $\lambda = 808$ nm and a power density of 7 W cm^{-2}. The sample was exposed from 0 to 120 s but not from 120 to 240 s. As shown in Figure 2b, the temperature of the PLGA–Au H-S NP solution (concentration of 145 μg mL^{-1}) increases linearly from 26.3 to 33.1°C ($\triangle T \approx 7$°C) under NIR irradiation. However, when the Au nanoparticle solution (2.7 mg mL^{-1}), the PLGA nanoparticle solution (3.3 mg mL^{-1}), and the deionized water are irradiated by NIR light, the temperature increases much less than that of the PLGA–Au H-S NP solution. These results confirm the photothermal conversion property of PLGA–Au H-S NPs. We have also studied the dependence of this property on the laser power density and the PLGA–Au H-S NP solution concentration. Higher power densities and nanoparticle concentrations are seen to result in larger increases in temperature (see the Supporting Information, Figure S1). It implies that $\triangle T$ can be controlled by adjusting NIR power density and nanoparticle concentration.

In in vitro release experiments, rhodamine-loaded PLGA–Au (25 nm) H-S NPs were prepared and the amount of released rhodamine was measured by using a UV spectrophotometer. The release profiles obtained with and without NIR irradiation are presented in Figure 3a. Drug release from PLGA particles generally shows a triphasic profile; an initial burst release, a lag phase, and a secondary burst with approximately zero-order release kinetics.[13] Since rhodamine used as the model drug is a fluorescent dye, we also monitored rhodamine release from PLGA nanoparticles by using total internal reflection fluorescence microscopy (TIRFM). Figure 3b and c shows TIRFM images of rhodamine-loaded PLGA–Au H-S NPs with and without NIR irradiation, respectively, for different times. The red circles correspond to rhodamine-encapsulated PLGA nanoparticles. The diameter of these red circles significantly decreases with increasing NIR irradiation time, and the peak emission intensity of a rhodamine-loaded PLGA nanoparticle is reduced approximately by an order of magnitude for 50 min (see the Supporting Information, Figure S2). On the other hand, the background intensity increases until 15 min and then decreases because of the diffusion of released rhodamine. However, when not exposed to NIR light, very little rhodamine seems to be released from PLGA nanoparticles within 50 min. These TIRFM data support photothermally controlled drug delivery.

Figure 4a–c shows field-emission scanning electron microscopy (FESEM) and transmission electron microscopy (TEM) images of rhodamine-loaded PLGA–Au H-S NPs before NIR irradiation, and after 2-, and 3-day exposure, respectively. After a 3-day irradiation, the PLGA uncovered with Au is rapidly degraded and only Au H-S NPs are left, whereas rhodamine-loaded PLGA–Au H-S NPs without irradiation maintain their shapes even after three days. These results are consistent with the in vitro release experiments in Figure 3a.

Besides morphology studies, we have further investigated the optical and photothermal conversion properties of rhodamine-loaded PLGA–Au H-S NPs with PLGA nanoparticles partially degraded by NIR irradiation. As shown in Figure 5a, the absorption peak is around 823 nm before NIR irradiation. However, the peak is shifted to shorter wavelengths with increasing NIR irradiation time and remains nearly unchanged after a 3-day irradiation. This finding indicates that the surface plasmon resonance peak of Au half-shells is about 783 nm because PLGA nanoparticles are completely degraded within 3 days under NIR irradiation. Figure 5b shows the time dependence of the temperature for the PLGA–Au H-S NP solution irradiated by NIR light from a laser diode at 808 nm. During the experiments, one-minute irradiation periods were repeated with a power density of 7 W cm^{-2}. At first, the temperature increases rapidly

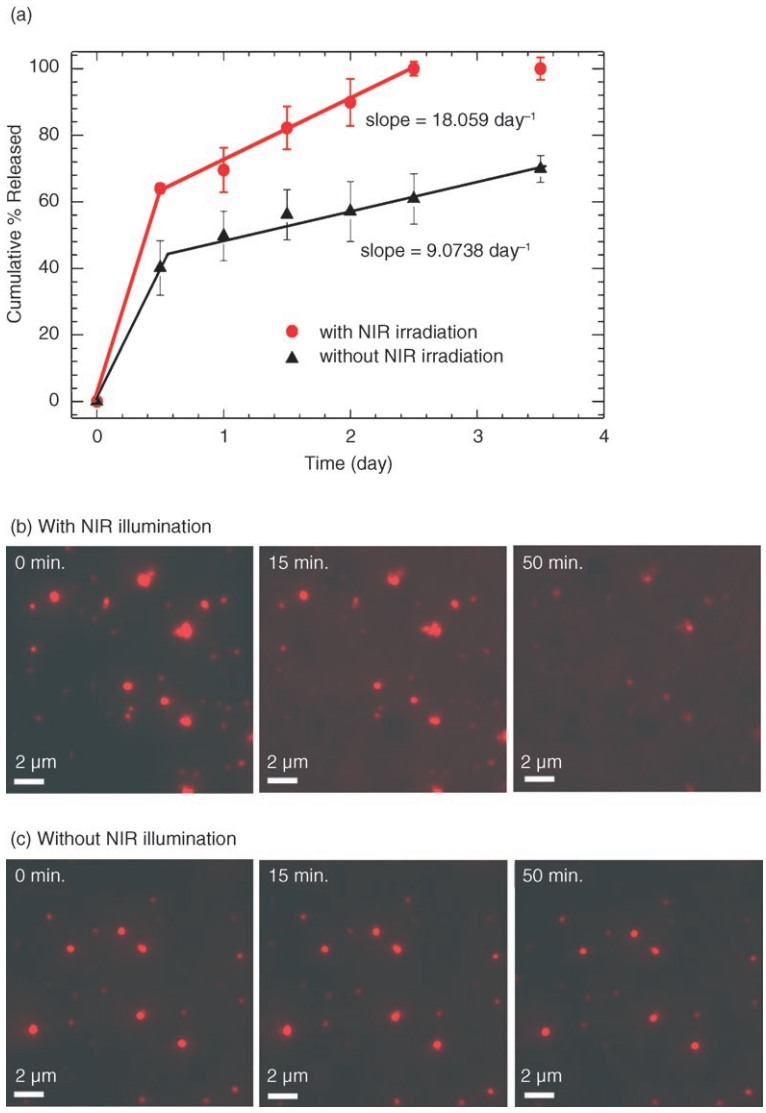

Figure 3. a) Rhodamine release profiles from PLGA nanoparticles (molecular weight, M_w = 20 000) with and without NIR irradiation. One-minute irradiation periods were repeated during the experiments with a power density of 7 W cm^{-2}. b,c) Evolution of TIRFM images as rhodamine is released from PLGA–Au H-S NPs during NIR irradiation using a 808-nm laser diode with a power density of 20 W cm^{-2} (b) and without NIR irradiation (c).

up to nearly 57°C with oscillations in response to the periodic NIR exposure. Then, the temperature remains constant for 3 days, although it decreases slightly because of the shift of the absorption peak.

Figure 6a shows the absorption spectra of PLGA–Mn/Au H-S NPs. For Mn (10 nm)/Au (0 nm), a surface plasmon resonance peak is not observed in the range 400–1100 nm. For Mn (10 nm)/Au (25 nm), however, the absorption peak is found at about 845 nm. The surface plasmon resonance peak of PLGA–Mn/Au H-S NPs is still in the NIR range in spite of the Mn layer, so that NIR light can be converted to thermal energy, as shown in the inset of Figure 5b. In Figure 6b and c, the spin–spin relaxation time (T_2)-weighted spin-echo MR images and $1/T_2$ measured at 1.5 T are shown as a function of nanoparticle concentration for PLGA–Mn (10 nm)/Au (25 nm) H-S NPs and PLGA–Au (25 nm) H-S NPs without a Mn layer. For the former, $1/T_2$ increases linearly with increasing nanoparticle concentration, whereas $1/T_2$ of nanoparticles without a Mn layer has the same value as that of water, independent of the concentration. These results suggest that PLGA–Mn/Au H-S NPs can be used as MRI contrast agents because of the Mn layer. In addition, we have also investigated the mobility of rhodamine-loaded PLGA–Mn/Au H-S NPs in an external magnetic field by a fluorescence microscope. The nanoparticles were observed to move in the direction of the magnetic field (see the Supporting Information, Movie S1). It indicates that drug-loaded PLGA–Mn/Au H-S NPs could possibly be used as magnetic drug carriers for targeted delivery.[14] For targeted drug delivery and MRI, the potential toxicity and cytotoxicity of PLGA–Mn/Au H-S NPs should be evaluated. However, since PLGA, Au, and Mn, which comprise these nanoparticles, appear biocompatible and non-cytotoxic as supported by recent experiments on human cells,[15,16] their toxicity is expected to be within a tolerable range.

In summary, we have developed NIR-resonant rhodamine-encapsulated PLGA–Mn/Au H-S NPs by depositing metal multilayers on PLGA nanoparticles and we have shown that these nanoparticles can be used for photothermally controlled drug delivery and MR imaging. The photothermal conversion in the Au layer has been investigated by measuring the temperature of the nanoparticle solution, and the temperature increase $\triangle T$ is observed to be dependent on NIR irradiation time, power density, and nanoparticle concentration. Upon NIR irradiation, the release rate of rhodamine from the PLGA nanoparticles is found to be about twice as great as the one without NIR irradiation; this photothermally controlled drug delivery has been confirmed through FESEM/TEM and TIRFM images and absorption spectra. Furthermore, if these nanoparticles are conjugated with targeting ligands, as reported by other

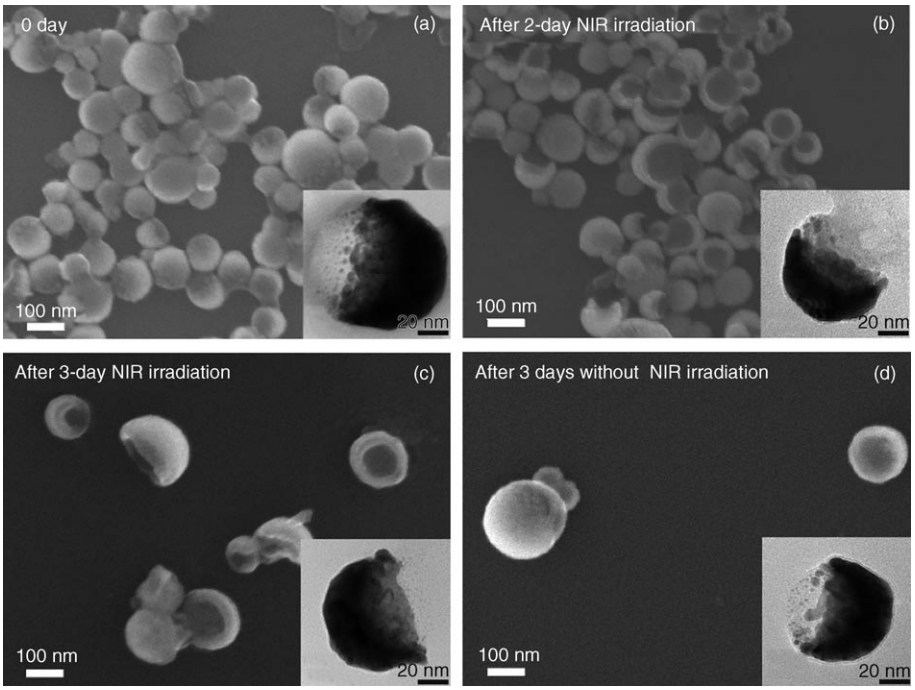

Figure 4. FESEM images of PLGA–Au H-S NPs right after fabrication (a), after 2-day NIR irradiation (b), after 3-day NIR irradiation (c), and in the water for three days without NIR irradiation (d). The insets are TEM images.

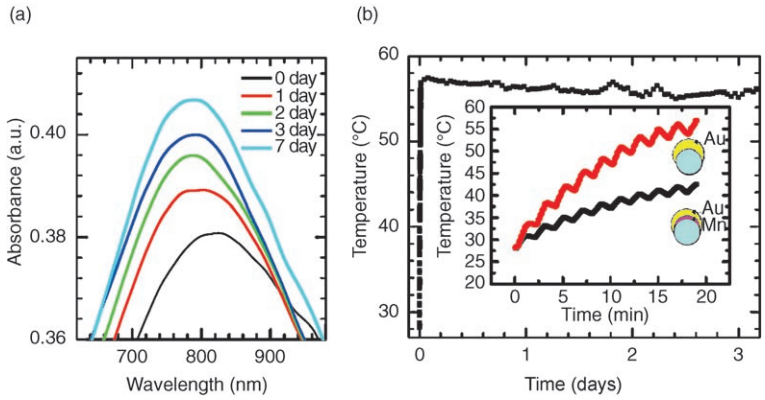

Figure 5. a) Absorption spectra for PLGA–Au H-S NPs irradiated for different time intervals. b) Temperature versus time for PLGA–Au H-S nanoparticle solution irradiated at 808 nm with a power density of 7 W cm^{-2}. The inset is temperature versus time during the first 20 min for PLGA–Au H-S NPs with a concentration of 200 μg mL^{-1} and PLGA–Mn/Au H-S NPs with a concentration of 100 μg mL^{-1}. During the experiments, one-minute irradiation periods were repeated.

groups,[17] selective cell targeting might possibly be achieved.

Experimental Section

Preparation and characterization of rhodamine-loaded PLGA nanoparticles: PLGA (100 mg, M_w = 20 000, Wako Chemicals) and rhodamine B (4 mg, M_w = 443, Sigma–Aldrich) were dissolved in a 50:50 ratio in 10 mL of chloroform. The organic solution was mixed with 20 mL of aqueous phase containing poly(vinyl alcohol) (2%, M_w = 15 000–20 000, Aldrich Chemical Co.) as a stabilizer. After the mutual saturation of organic and continuous phases, the mixture was emulsified for 10 min by ultrasonication at 250 W. The organic solvent was evaporated and the rhodamine-loaded PLGA nanoparticles were purified by centrifugation at 20 000 rpm for 30 min. The size of the nanoparticles, determined by dynamic light scattering (DLS), was approximately (75 ± 12) nm in diameter, and their glass transition temperature, measured by a differential scanning calorimetry (TA Instrument, SDT-600) was about 42 °C.

The amount of encapsulated rhodamine was measured as follows: The dried PLGA nanoparticles were mixed in phosphate buffer solution (pH 7.4). This suspension was then stirred and sonicated to extract rhodamine from the nanoparticles. After centrifugation, the amount of rhodamine loaded in the PLGA nanoparticles was measured using a UV spectrometer (Optizen 2120UV, MECASYS Co.). The encapsulation efficiency, which is defined as the percentage of the actual mass of drug encapsulated in the PLGA polymer relative to the initial amount of drug loaded, was estimated to be about 4.5%.

Fabrication of PLGA–metal multilayer H-S NPs: PLGA–metal multilayer H-S NPs are fabricated by depositing thin metal layers onto monolayers of PLGA nanoparticles, which were prepared by spin-casting aqueous suspensions of nanoparticles onto a silicon substrate.[18,19] After the deposition of the metal films, metal-deposited polymer nanoparticles were released into water from the substrate surface by sonication and collected by centrifugation.

Measurements of photothermal conversion properties: 4 mL of PLGA–Au (25 nm) H-S NP solution was prepared in a transparent vial. The temperature of the solution was measured using a thermocouple, while it was irradiated with a 808-nm coherent diode laser (Unique mode 30k/400/20 (808 ± 3) nm, Jenoptik

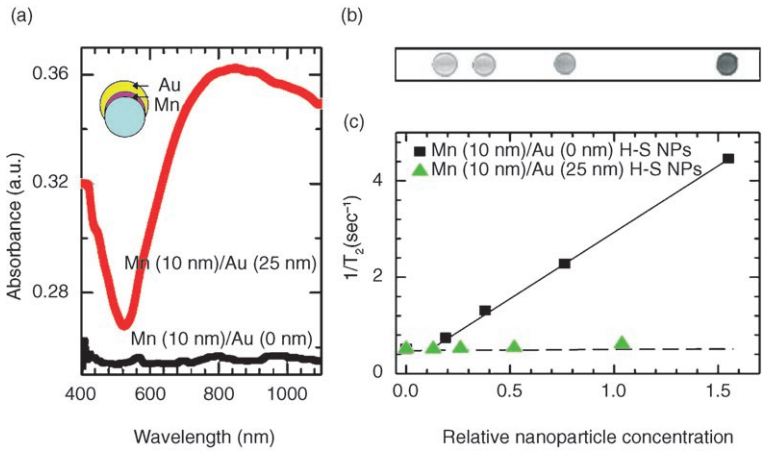

Figure 6. a) Absorption spectra for PLGA–Mn (10 nm)/Au (0, 25 nm) H-S NPs. b) T_2-weighted images of PLGA–Mn (10 nm)/Au (25 nm) H-S NPs for different nanoparticle concentrations. c) $1/T_2$ versus relative nanoparticle concentration for PLGA–Mn (10 nm)/Au (25 nm) and PLGA–Mn (0 nm)/Au (25 nm) H-S NPs.

Co.) for 2 min. In order to investigate the dependence of laser power density and nanoparticle concentration on photothermal conversion properties, the laser power density was varied from 7 to 25 W cm^{-2} and the nanoparticle concentration was varied from 36.25 to 145 μg mL^{-1}.

In vitro release experiments: 5 mL of rhodamine-encapsulated PLGA–Au (25 nm) H-S NP solution with a concentration of about 200 μg mL^{-1} was loaded into a 10 000 Dalton molecular-weight cut-off membrane dialysis tube. The tube was immersed in a transparent vial filled with 4 mL of phosphate buffer solution (pH 7.4, 10 mM) during release experiments. The release experiments were performed with and without NIR irradiation at room temperature. During the experiments, one-minute irradiation periods were repeated with a power density of 7 W cm^{-2}. The amount of released rhodamine was measured through UV absorbance. All measurements were conducted in triplicate.

Total internal reflection fluorescence microscopy experiments: TIRF microscopy was performed with a Nikon Eclipse TE2000 inverted fluorescence microscope (Nikon, Melville, NY, USA) equipped with a 532 nm laser (CrystaLaser, Reno, NV, USA) and a digital camera C9100 EM-CCD (Hamamatsu, Bridgewater, NJ, USA). The output power of the laser was 200 mW. The microscope uses a CFI Apochromat oil-immersion objective (100×, numerical aperture, NA = 1.49) and detects with a filter set (EX: 510–560 nm, DM: 570 nm, and BA: 590 nm). The sample stage index-matched custom-made glass bottom well dishes were from MaTek cultureware (Ashland, MA, USA). The filter set and the camera were controlled by Metamorph software (Universal Imaging, Downingtown, PA, USA). Release images were captured every five minutes for an hour with an exposure time of 1 ms. The NIR irradiation was maintained during the experiments with the power density of 20 W cm^{-2}.

Keywords:
contrast enhancement · core/shell materials · encapsulation · gold · magnetic resonance imaging

[1] R. D. Averitt, D. Sarka, N. J. Halas, *Phys. Rev. Lett.* **1997**, *78*, 4217–4220.
[2] C. Loo, A. Lin, L. Hirsh, M.-H. Lee, J. Barton, N. Halas, J. West, R. Drezek, *Technol. Cancer Res. Treat.* **2004**, *3*, 33–40.
[3] L. R. Hirsh, R. J. Stafford, J. A. Bankson, S. R. Sersher, B. Rivera, R. E. Price, J. D. Hazle, N. J. Halas, *Proc. Natl. Acad. Sci. USA* **2003**, *100*, 13549–13554.
[4] S. R. Sershen, S. L. Westcott, N. J. Halas, J. L. West, *J. Biomed. Mater. Res.* **2000**, *51*, 293–298.
[5] S. R. Sershen, S. L. Westcott, N. J. Halas, J. L. West, *Appl. Phys. Lett.* **2002**, *80*, 4609–4611.
[6] C. Loo, A. Lowery, N. Halas, J. West, R. Drezek, *Nano Lett.* **2005**, *5*, 709–711.
[7] J. Chen, F. Saeki, B. J. Wiley, H. Chang, M. J. Cobb, Z.-Y. Li, L. Au, H. Zhang, M. B. Kimmey, X. Li, Y. Xia, *Nano Lett.* **2005**, *5*, 473–477.
[8] Z. Liu, H. Song, L. Yu, L. Yang, *Appl. Phys. Lett.* **2005**, *86*, 113 109–113 112.
[9] X. Huang, I. H. El-Sayed, W. Qian, M. A. El-Sayed, *J. Am. Chem. Soc.* **2006**, *128*, 2115–2120.
[10] H. Takahash, J. Niidome, A. Nariai, Y. Niidome, S. Yamada, *Chem. Lett.* **2006**, *35*, 500–501.
[11] J. Kim, S. Park, J. E. Lee, S. M. Jin, J. H. Lee, I. S. Lee, I. Yang, J.-S. Kim, S. K. Kim, M.-H. Cho, T. Hyeon, *Angew. Chem. Int. Ed.* **2006**, *45*, 7754–7758.
[12] R. W. Rowe-Horwege, *Systemic Hyperthermia in Encyclopedia of Medical Devices and Instrumentation*, 2nd Ed. (Ed: J. G. Webster), John Wiley and Sons, New York **2006**, pp. 42–62.
[13] B. S. Zolink, P. E. Leary, D. J. Burgess, *J. Controlled Release* **2006**, *112*, 293–300.
[14] L. E. Udrea, N. J. C. Strachan, V. Badescu, O. Rotariu, *Phys. Med. Biol.* **2006**, *51*, 4869–4881.
[15] E. E. Connor, J. Mwamuka, A. Gole, C. J. Murphy, M. D. Wyatt, *Small* **2005**, *1*, 325–327.
[16] H. B. Na, J. H. Lee, K. An, Y. I. Park, M. Park, I. S. Lee, D. Nam, S. T. Kim, S. Kim, S. Kim, K. Lim, K. Kim, S. Kim, T. Hyeon, *Angew. Chem. Int. Ed.* **2007**, *46*, 5397–5401.
[17] M. V. Yezhelyev, X. Gao, Y. Xing, A. Al-Hajj, S. Nie, R. M. O'Regan, *Lancet Oncol.* **2006**, *7*, 657–667, and references therein.
[18] J. C. Love, B. D. Gates, D. B. Wolfe, K. E. Paul, G. M. Whitesides, *Nano Lett.* **2002**, *2*, 891–894.
[19] Y. Lu, G. L. Liu, J. Kim, Y. X. Mejia, L. P. Lee, *Nano Lett.* **2005**, *5*, 119–124.

Received: September 5, 2007
Revised: December 12, 2007
Published online on January 18, 2008